Analysis of ^{7}Li(n, n')^{7}Li* reactions using the continuum-discretized coupled-channels method

D. Ichinkhorloo,[1,*] Y. Hirabayashi,[2] K. Katō,[3] M. Aikawa,[3] T. Matsumoto,[4] and S. Chiba[5]
[1]*Meme Media Laboratory, Hokkaido University, Sapporo 060-8628, Japan*
[2]*Information Initiative Center, Hokkaido University, Sapporo 060-0810, Japan*
[3]*Nuclear Reaction Data Centre, Faculty of Science, Hokkaido University, Sapporo 060-0810, Japan*
[4]*Department of Physics, Kyushu University, Fukuoka 812-8581, Japan*
[5]*Research Laboratory for Nuclear Reactors, Tokyo Institute of Technology, Tokyo 152-8550, Japan*
(Received 30 October 2012; published 11 December 2012)

We study ^{7}Li(n, n')^{7}Li* reactions by using the continuum-discretized coupled-channels (CDCC) method with the complex Jeukenne-Lejeune-Mahaux effective nucleon-nucleon interaction. In this study, the ^{7}Li nucleus is described by an $\alpha + t$ cluster model. The calculated elastic cross sections for incident energies between 11.5 and 24.0 MeV show good agreements with experimental data. Furthermore, we calculate the neutron spectra of ^{7}Li ground and excited breakup states measured at selected angular points for incident energies of 11.5 and 18.0 MeV. The results reproduce the observed data systematically.

DOI: 10.1103/PhysRevC.86.064604 PACS number(s): 24.10.Eq, 25.40.Fq, 21.60.Gx, 27.20.+n

I. INTRODUCTION

The breakup of lithium isotopes and their inverse reactions in the low relative energy region are of a great interest from the astrophysics point of view, because the radiactive capture reactions at very low energies ($E_{cm} \leqslant$ 10–100 keV) are one of the key reactions in the nucleosynthesis in the early Universe and during stellar evolution [1]. The n + Li reactions are important not only due to basic research interest but also from the application point of view. Lithium isotopes will be used as a tritium-breeding material in d-t fusion reactors. Therefore accurate nuclear data are required for n- and p-induced reactions. Indeed, the International Atomic Energy Agency (IAEA) is organizing a research coordination meeting to prepare nuclear data libraries for advanced fusion devices, FENDL-3, and the maximum incident energy is set at 150 MeV to comply fully with the requirements for the International Fusion Materials Irradiation Facility (IFMIF) design [2]. Lithium isotopes are some of important materials in these libraries.

In spite of the importance of the n + Li reactions as described above, experimental data leading to Li continuum breakup processes are extremely rare for the neutron energy region above 20 MeV [3–7]. Furthermore, the statistical model, used often in evaluation of nuclear data for medium to heavy nuclei, cannot be applied to the Li(n, n') reactions, as mentioned in Refs. [8,9]. It is difficult to calculate cross section data for the Li(n, n') reaction because the reaction mechanisms leading to three- or four-body final states are not understood well enough for nuclear data evaluation. Therefore more reliable theoretical calculations for the cross sections are highly desirable.

As one of the most reliable methods for treating breakup processes, the continuum-discretized coupled-channels (CDCC) method [10] has been proposed and successfully applied to analyses of three-body breakup systems, in which the projectile breaks up into two constituents, such as ^{7}Li (^{6}Li) into t (d) and α. For CDCC analyses of Li elastic and inelastic scattering on various targets, Sakuragi *et al.* [11] have reproduced the absolute values of a lot of experimental data of cross sections very well.

Furthermore, the CDCC method has been also applied to the sequential Coulomb nuclear breakup via the resonance state of Li, in which both Coulomb and nuclear breakup processes were taken into account consistently [12]. Thus, the CDCC method is expected to be indispensable to analyze Li breakup reactions.

In the previous work [13], we have successfully studied n + ^{6}Li reactions by applying the CDCC method with an $\alpha + d + n$ model. However, the CDCC method has not been confirmed to be applicable to breakup of continuum states of ^{7}Li, and especially to breakup spectra of ^{7}Li. Furthermore, ^{7}Li is the major tritium breeding material, in addition to ^{6}Li, and is by far the most common isotope of natural Li (92.5%). The structure of ^{7}Li is simpler than ^{6}Li. This is a basic interest of the theoretical framework to describe reaction mechanisms relevant to breakup processes. In addition, the ^{7}Li nucleus is known to have a well developed $\alpha + t$ cluster structure and the binding energy is very small 2.467 MeV from the threshold [11].

In this paper, cross sections for elastic and inelastic neutron scattering of ^{7}Li reactions are evaluated by using the CDCC method [11], in which we adopt wave functions of ^{7}Li constructed by the $\alpha + t$ model and a microscopic Jeukenne-Lejeune-Mahaux (JLM) effective nucleon-nucleon interaction [14] to calculate potentials between n and ^{7}Li by the folding procedure.

This paper is organized as follows. We describe the CDCC method including calculations of ^{7}Li wave functions and coupling potentials with the JLM interaction in Sec. II. We present the calculated results and discuss the applicability in Sec. III. Finally, we give a summary in Sec. IV.

*ichinkhorloo@nucl.sci.hokudai.ac.jp

II. THE METHOD

A. Formulation

The wave function of ^{7}Li based on the α-t cluster model is expressed as

$$\Phi_\ell^{Im}(\boldsymbol{\xi}) = \psi_\ell^{Im}(\boldsymbol{r})\varphi(\alpha)\varphi(t), \tag{1}$$

where $\boldsymbol{r}$ and $\boldsymbol{\xi}$ are the relative coordinate between α and t and a set of internal coordinates of ^{7}Li, respectively. Here, the internal ground-state wave functions of α and t are expressed by $\varphi(\alpha)$ and $\varphi(t)$, respectively, where $\varphi(t)$ does not include a spin degree of freedom in a triton. The α-t relative wave function ψ_ℓ^{Im} with the orbital angular momentum ℓ, total spin I, and its projection m on the z axis can be described as

$$\psi_\ell^{Im}(\boldsymbol{r}) = \phi_\ell^I(r)[i^\ell Y_\ell(\Omega_r) \otimes \eta_t]_{Im}, \tag{2}$$

where $\phi_\ell^I(r)$ is the radial part of the relative wave function of ^{7}Li, and η_t is the spin wave function of a triton with spin 1/2. In the present calculation, we prepare the Hamiltonian $H(^7\mathrm{Li})$ for the relative motion of α and t in ^{7}Li, which is shown to reproduce the experimental data of the ground state (-2.47 MeV) and the $7/2^-$ resonance state (2.20 MeV) as well as the low-energy part of observed α-t scattering phase shifts.

In the CDCC method, the relative wave functions of ^{7}Li for continuum states in addition to the bound states, including the ground and $1/2^-$ excited states, are given by a sum of a finite number of discretized states denoted by

$$\hat{\psi}_{i\ell}^{Im}(\boldsymbol{r}) = \hat{\phi}_{i\ell}^I(r)[i^\ell Y_\ell(\Omega_r) \otimes \eta_t]_{Im} \quad (i = 0\text{–}N_{\ell,I}), \tag{3}$$

whose energies $\varepsilon_{i\ell}^I$ are given by

$$\varepsilon_{i\ell}^I = \langle \hat{\psi}_{i\ell}^{Im}(\boldsymbol{r}) | H(^7\mathrm{Li}) | \hat{\psi}_{i\ell}^{Im}(\boldsymbol{r}) \rangle. \tag{4}$$

This is the energy of ^{7}Li measured from the α and t thresholds.

As a discretization approach, we adopt here the pseudostate method [15–17] instead of the momentum bin method. The advantage of the pseudostate method is that, if there are resonances in its excitation spectrum, we can describe discretized continuum states with a reasonable number of the basis functions, without distinguishing the resonance states from nonresonant continuous states as mentioned in Ref. [16]. As is well known, two resonances in $\ell = 3$ are observed in ^{7}Li. Therefore the pseudostate method is very useful for analyses of ^{7}Li breakup reactions.

In the pseudostate method, we diagonalize $H(^7\mathrm{Li})$ in a space spanned by a finite number of L^2-type basis functions for r, $\{\varphi_{j\ell}\}$, and discretized wave functions $\hat{\phi}_{i\ell}^I$ for the radial part are obtained by

$$\hat{\phi}_{i\ell}^I(r) = \sum_{j=1}^{j_{\max}} A_{j\ell}^I \varphi_{j\ell}(r). \tag{5}$$

As the basis functions, complex-range Gaussian basis functions [16,18] are adopted, and we include $\ell = 0, 1, 2$, and 3 for the relative angular momenta of α-t: ^1S, ^1P, ^3P, ^3D, ^5D, ^5F, and ^7F represent the S, P, D, and F wave states with $1/2^+$, $1/2^-$, $3/2^-$ $3/2^+$, $5/2^+$, $5/2^-$, and $7/2^-$, respectively. The number of states $N_{\ell,I}$ is chosen to involve all open channels for each incident energy.

The $n + {}^7$Li scattering can be described as a three-body system, $n + \alpha + t$. The Schrödinger equation is written as

$$\left[K_R + \sum_{j\in{}^7\mathrm{Li}} v_{j0} + H(^7\mathrm{Li}) - E \right] \Psi(\boldsymbol{\xi}, \boldsymbol{R}) = 0, \tag{6}$$

where E is the energy of the total system, and $\boldsymbol{R}$ represents a coordinate between n and the center of mass of ^{7}Li. K_R is a kinetic energy operator associated with $\boldsymbol{R}$, and an effective interaction between the jth nucleon in ^{7}Li and the incident n is represented by v_{j0}. The total wave function with the total angular momentum J and its projection M on the z-axis, Ψ_{JM}, is expanded in terms of the orthonormal set of eigenstates of $H(^7\mathrm{Li})$ which is the Hamiltonian of the α-t system: After the discretization and the truncation of α-t continuum, Ψ_{JM} is reduced to an approximate one,

$$\begin{aligned}\Psi_{JM}^{\mathrm{CDCC}} = &\sum_L \mathcal{Y}_{JM}^{\gamma_{3/2^-}} \hat{\phi}_{01}^{3/2^-}(r)\hat{\chi}_{\gamma_{3/2^-}}(\hat{P}_{\gamma_{3/2^-}}, R)/R \\ &+ \sum_L \mathcal{Y}_{JM}^{\gamma_{1/2^-}} \hat{\phi}_{01}^{1/2^-}(r)\hat{\chi}_{\gamma_{1/2^-}}(\hat{P}_{\gamma_{1/2^-}}, R)/R \\ &+ \sum_\gamma^{\gamma_{\max}} \mathcal{Y}_{JM}^{\ell IL} \hat{\phi}_{i\ell}^I(r)\hat{\chi}_\gamma(\hat{P}_\gamma, R)/R,\end{aligned} \tag{7}$$

where

$$\mathcal{Y}_{JM}^{\ell IL} = [[i^\ell Y_\ell(\Omega_r) \otimes \eta_t]_I \otimes i^L Y_L(\Omega_R)]_{JM}\varphi(\alpha)\varphi(t). \tag{8}$$

Here $\gamma_{3/2^-} = (0, 1, 3/2, L, J)$, $\gamma_{1/2^-} = (0, 1, 1/2, L, J)$, and $\gamma = (i, \ell, I, L, J)$ represent the elastic, inelastic, and breakup channels, respectively. The expansion coefficient $\hat{\chi}_\gamma$ in Eq. (7) represents the relative motion between n and ^{7}Li, and L is the orbital angular momentum. The number $\gamma_{\max}$ represents the size of the model space and is discussed in the next subsection.

The relative momentum P_γ is determined by conservation of the total energy,

$$E = \hat{P}_\gamma^2/2\mu + \varepsilon_{i\ell}^I, \tag{9}$$

with μ being the reduced mass of the $n + {}^7$Li system. Multiplying Eq. (6) by $[\hat{\phi}_{i\ell}^I(r)\mathcal{Y}_{JM}^{\ell IL}]^*$ from the left-hand side and integrating over the degrees of freedom except for R, one can obtain a set of coupled differential equations for $\hat{\chi}_\gamma$, called the CDCC equation. Solving the CDCC equation under the appropriate asymptotic boundary condition, we can obtain the elastic and discrete breakup S-matrix elements. Details of the formalism of the CDCC method are shown in Ref. [10].

B. Discretized states of ^{7}Li and the model space of $n + {}^7$Li

The Hamiltomian $H(^7\mathrm{Li})$ for relative motion between α and t in ^{7}Li is given as

$$H(^7\mathrm{Li}) = K_r + v_{\alpha t}(r), \tag{10}$$

where the K_r is a kinetic energy, and the interaction $v_{\alpha t}(r)$ between α and t is chosen in a way similar to that of Sakuragi *et al.* [11]. In this calculation, the Pauli forbidden states are defined by the harmonic oscillator wave function $u_{i\ell}^{PF}(r, \nu)$

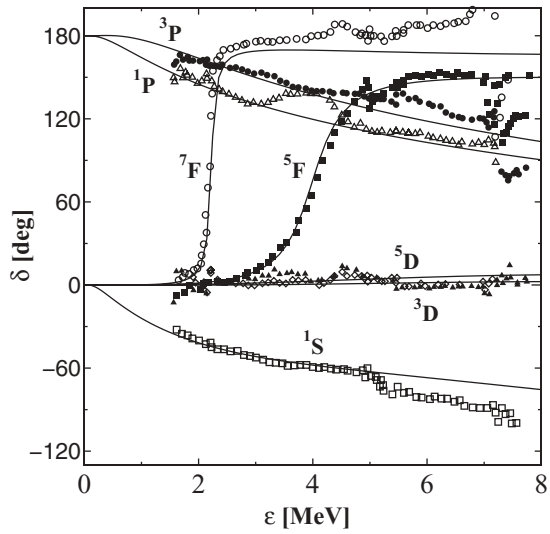

FIG. 1. α-t scattering phase shifts for $\ell = 1$ $(3/2^-, 1/2^-)$, $\ell = 0$ $(1/2^+)$, $\ell = 2$ $(3/2^+, 5/2^+)$, and $\ell = 3$ $(5/2^-, 7/2^-)$. The solid lines are given by our calculation with the α-t cluster model. The experimental data are taken from Ref. [20].

with the total oscillator quanta $N \leqslant 2$ and the oscillator constant $\nu = 0.8$ fm^{-2}. We solve the Schrödinger equation with the orthogonality condition model [19],

$$H(^7\mathrm{Li})\hat{\phi}^I_{i\ell}(r) = \varepsilon^I_{i\ell}\hat{\phi}^I_{i\ell}(r), \tag{11}$$

$$\left\langle \hat{\phi}^I_{i\ell}(r) \middle| u^{PF}_{i\ell}(r, \nu) \right\rangle = 0, \tag{12}$$

where the number of the basis function is $j_{\max} = 20$.

The potential $\upsilon_{\alpha t}(r)$ is expressed as

$$\upsilon_{\alpha t}(r) = V_{\mathrm{eff}}(r) + a_{I\ell} V^{(SO)}_{\mathrm{eff}}(r), \tag{13}$$

and

$$\begin{aligned} V_{\mathrm{eff}}(r) &= \upsilon_{1,\ell} e^{-(r/r_{1,\ell})^2} + \upsilon_{2,\ell} e^{-(r/r_{2,\ell})^2} + V_{CL}(r), \\ V^{(SO)}_{\mathrm{eff}}(r) &= \upsilon^{(SO)}_{1,\ell} e^{-(r/r^{(SO)}_{1,\ell})^2} + \upsilon^{(SO)}_{2,\ell} e^{-(r/r^{(SO)}_{2,\ell})^2}, \end{aligned} \tag{14}$$

where $a_{I\ell} = \{I(I+1) - \ell(\ell+1) - 3/4\}/2$ and $V_{CL}(r)$ is the Coulomb potential given in Ref. [11]. The potential parameters are chosen ℓ-dependently so as to reproduce well the energies of the ground and the first excited states, and the α-t scattering phase shifts as shown in Fig. 1. It is well known that the effective α-t potential has remarkable parity dependence [11]. Keeping this in mind and taking into account the orthogonality condition model different treatment of the Pauli forbidden states in the present calculation and in Ref. [11], we parametrize the effective central potential and the spin-orbit potential with a two-range Gaussian form for $\ell = 0$, 1, 2, and 3. The parameters are listed in Table I.

We prepare the wave functions of the two bound and discretized α-t scattering solutions for ^{7}Li with S wave $(\ell = 0)$, P wave $(\ell = 1)$, D wave $(\ell = 2)$, and F wave $(\ell = 3)$; the spin of triton couples and composes the total spins $J^\pi = 1/2^+, 3/2^-, 1/2^-, 3/2^+, 5/2^+, 5/2^-$, and $7/2^-$, respectively. We note here that the two-bound states are the $3/2^-$ ground state (gr.s.) at $\varepsilon^{3/2}_{0,1} = -2.47$ MeV and the $1/2^-$ first excited state (ex.s.) at $\varepsilon^{1/2}_{0,1} = -1.98$ MeV. The $7/2^-$ and $5/2^-$ states have resonant states at $\varepsilon^{7/2}_{5,3} = 2.20$ MeV (R) and $\varepsilon^{5/2}_{8,3} = 4.05$ MeV (R), respectively, where these two are regarded as the doublet of the α-t resonance states in the F wave. There are no resonances in the S, P, and D waves. Next, we solve the coupled-channel equation of Eq. (6), employing the discretized solutions for ^{7}Li. The model space expressed by Eq. (7) is truncated by $\gamma_{\max}$, which is described with $\varepsilon^I_{i\ell} < \varepsilon_{\max}$ $(= \hbar^2 k^2_{\max}/2\mu_{\alpha t}$, $k_{\max} = 1.0$ fm$^{-1})$ for the discretized continuum energy of ^{7}Li. We divide the S, P, D, and F wave continua into $N_{\ell=0,I} = 12$, $N_{\ell=1,I} = 14$, $N_{\ell=2,I} = 12$, and $N_{\ell=3,I} = 13$ numbers of the states, respectively. Level sequences of the resulting discrete eigenstates are shown in Fig. 2.

C. Coupling potentials

For the calculation of diagonal and coupling potentials in the CDCC equation, we use the complex Jeukennd-Lejeune-Mahaux (JLM) effective nucleon-nucleon interaction [14] based on a single folding model. The JLM interaction can be easily applied to coupled-channels calculations of nucleon-nucleus systems, such as in Refs. [21,22]. This interaction has energy and density dependence, and forms a Gaussian with both real and imaginary parts,

$$\begin{aligned} \upsilon_{j0}(R_{j0}; \rho, E) = \lambda_v V(\rho, E) \exp\left(-R_{j0}/t_R^2\right) \\ + i\lambda_w W(\rho, E) \exp\left(-R_{j0}/t_I^2\right), \end{aligned} \tag{15}$$

where R_{j0} is a coordinate of the jth nucleon in ^{7}Li and the incident neutron n is described by the suffix 0. The parameters, t_R, t_I, and λ_v, are taken as the same ones used in the

TABLE I. The parameters of the effective centrel and spin orbit potentials between α and t for $\ell = 0$, 1, 2 and 3

Parameters	$\ell = 0$	$\ell = 1$ $(3/2^-)$	$\ell = 1$ $(1/2^-)$	$\ell = 2$	$\ell = 3$
$\upsilon_{1,\ell}$ (MeV)	−119.38	−84.7	−89.5	−87.0	−75.65
$\upsilon_{2,\ell}$ (MeV)	13.78				
$\upsilon^{(SO)}_{1,\ell}$ (MeV)		−0.99	−0.3	−0.4	−1.05
$\upsilon^{(SO)}_{2,\ell}$ (MeV)		−0.67	−0.11		
$r_{1,\ell}$ (fm)	2.23	2.447	2.447	2.231	2.608
$r_{2,\ell}$ (fm)	3.310				
$r^{(SO)}_{1,\ell}$ (fm)		4.90	4.90	2.466	2.466
$r^{(SO)}_{2,\ell}$ (fm)		2.447	2.447		

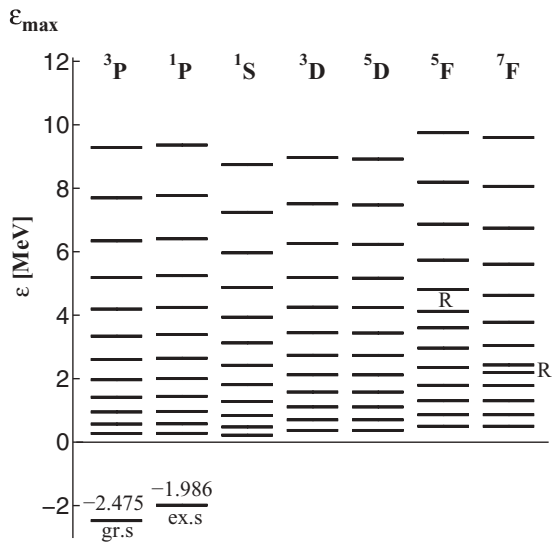

FIG. 2. The discretized eigenstates for ^{7}Li. Each panel indicated as ^3P, ^1P, ^1S, ^3D, ^5D, ^5F, and ^7F, from left to right sides correspond to $3/2^-$, $1/2^-$, $1/2^+$, $3/2^+$, $5/2^+$, $5/2^-$, and $7/2^-$, respectively. "R" indicates a resonant state.

original paper [14], $t_R = t_I = 1.2$, and $\lambda_v = 1.0$. Meanwhile the normalization for the imaginary part, λ_w, is optimized to reproduce the elastic cross sections, because the strength corresponding to the loss of flux depends on the model space considered in the calculation. Details for strengths of $V(\rho, E)$ and $W(\rho, E)$ are shown in Ref. [14].

Using the JLM interaction, the diagonal and coupling potentials, $V_{\gamma\gamma'}$, are obtained by

$$V_{\gamma\gamma'}(R) = \int \rho_{\gamma\gamma'}(\boldsymbol{s}, \Omega_R) v_{j0}(\boldsymbol{R}_{j0}, \bar{\rho}, E) d\boldsymbol{s} d\Omega_R, \quad (16)$$

where transition densities, $\rho_{\gamma\gamma'}$, and averaged matter density, $\bar{\rho}$, of ^{7}Li between γ and γ' are defined by

$$\rho_{\gamma\gamma'}(\boldsymbol{s}, \Omega_R) = \left\langle \mathcal{Y}^{\ell I L}_{JM} \hat{\phi}^I_{i\ell} \right| \sum_{j \in {}^7\mathrm{Li}} \delta(\boldsymbol{s} - \boldsymbol{s}_j) \left| \mathcal{Y}^{\ell' I' L'}_{JM} \hat{\phi}^{I'}_{i'\ell'} \right\rangle_{\hat{\boldsymbol{s}}},$$

and

$$\bar{\rho}(s) = \frac{1}{2} \int \{\rho_{\gamma\gamma}(\boldsymbol{s}, \Omega_R) + \rho_{\gamma'\gamma'}(\boldsymbol{s}, \Omega_R)\} d\Omega_s d\Omega_R, \quad (17)$$

respectively. Here s_j is a coordinate of the jth particle in ^{7}Li relative to the center of mass of ^{7}Li.

III. RESULTS AND DISCUSSION

Figure 3 shows the differential cross sections for the sum of the elastic and inelastic scattering to the first excited state of the $n + {}^7$Li reaction with incident energies between 11.5 and 24.0 MeV. One sees that the results of the full channel CDCC calculation represented by the solid lines are in good agreements with the experimental data. The dotted lines represent results of a one-channel calculation, in which the only ground state of ^{7}Li is taken into account. It is found that breakup effects shown by the difference between the

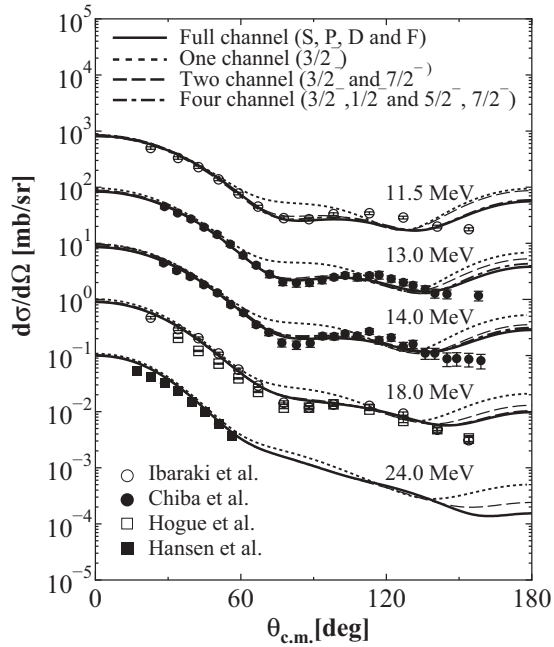

FIG. 3. Angular distribution of the differential cross sections for the sum of the elastic scattering and inelastic one to the first excited state of the $n + {}^7$Li reaction for incident energies between 11.0 and 18.0 MeV. The solid, dashed, dotted, and dash-dotted lines correspond to the results with and without couplings to breakup states of ^{7}Li, respectively. Experimental data are taken from Refs. [3,5–7]. The data are subsequently shifted downward by a factor of 10^{-1}–10^{-4} from 13.0 MeV to 24.0 MeV, respectively.

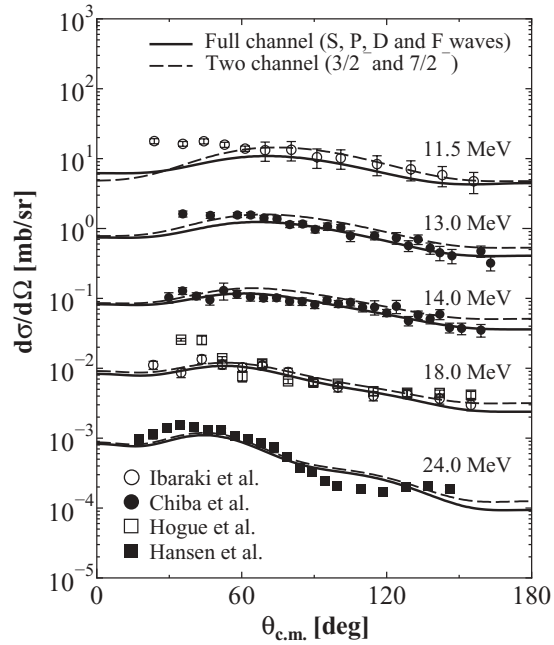

FIG. 4. Neutron inelastic scattering angular distribution to the $7/2^-$ resonance state 4.63 MeV above the α-t threshold. The experimental data are taken from Ref. [3,5–7]. The data for 13.0, 14.1, 18.0, and 24.0 MeV are shifted by factors of 0.1, 0.01, 0.001, and 0.0001, respectively.

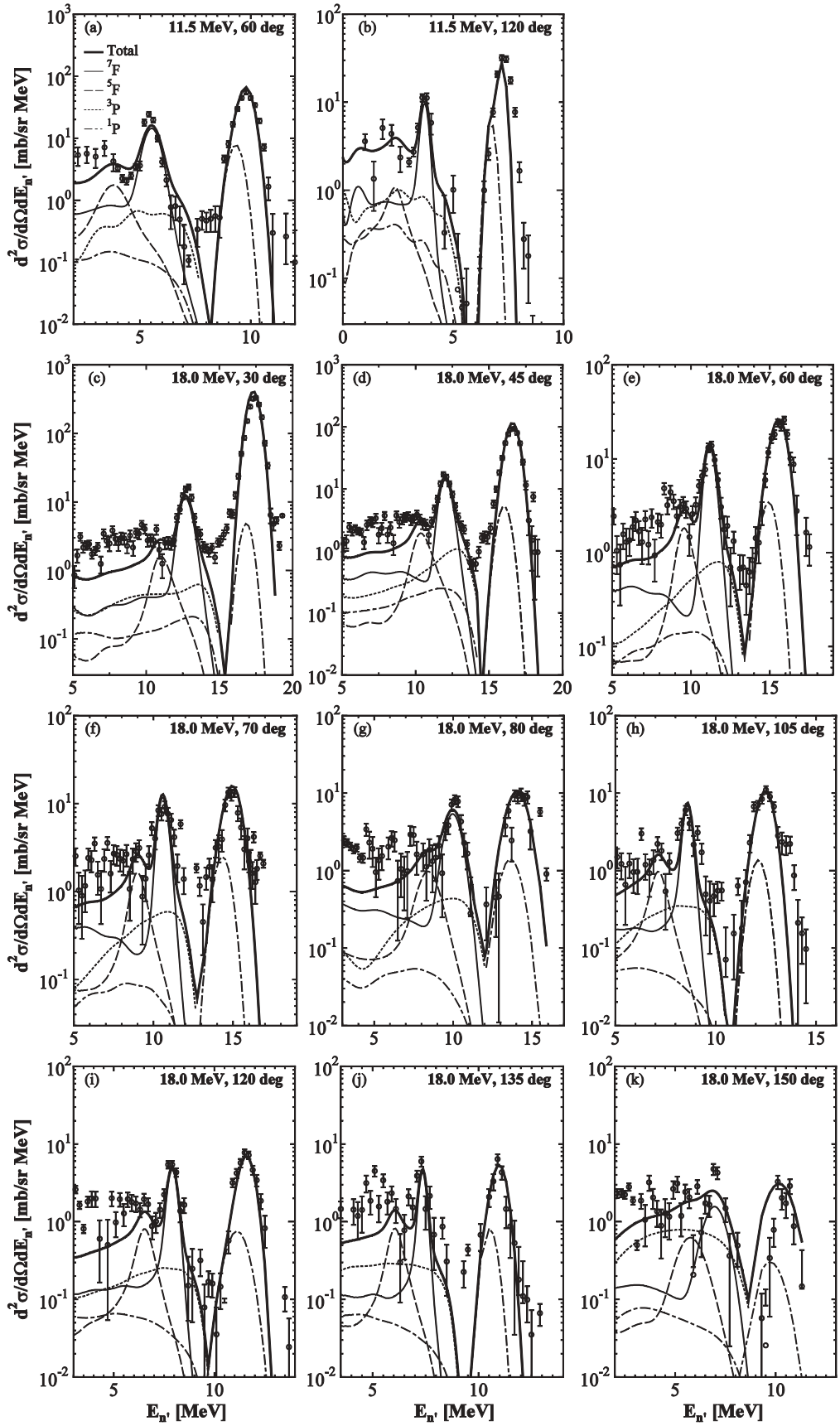

FIG. 5. The neutron spectra calculated by the CDCC method with the JLM interaction comparing with measured data at selected angular points in the laboratory system. The experimental data are taken from Ref. [8].

dotted and solid lines are significant enough to reproduce the angular distributions of the elastic scattering. The dashed lines represent two-channel results including the ground state $3/2^-$ and the $7/2^-$ resonance state. We can see large differences between dotted and dashed lines, and also see small differences between dashed and solid lines. This shows the most important contribution of the $7/2^-$ resonance state among the whole part of the ^{7}Li breakup effects to the elastic scattering. Four-channel calculations corresponding to dash-dotted lines include $3/2^-$ ground, $1/2^-$ bound, and $5/2^-$, $7/2^-$ resonance states. We show a small contribution of $1/2^-$ and $5/2^-$ resonant breakup states in comparison with the dashed line. Furthermore, it is interesting to note that the nonresonant breakup state contribution effect seems to depend on the incident energies in comparing the difference between dotted and solid lines and between dashed and solid lines. We also confirm a negligible contribution of the opposite parity breakup states (S wave and D wave) which have been suggested in the case of ^{6}Li scattering [11,23].

For all incident energies, we take $\lambda_w = 0.1$ to reproduce the angular distribution data for the elastic scattering. The main component of the flux loss from the elastic channel is considered to be due to breakups of ^{7}Li to t and α, which can be taken into account in the CDCC calculation directly. The other effects of the flux loss, such as the excitation of α and t breakup, are not so large because of low incident energies. Therefore the strength of λ_w becomes very small. Here, it should be noted that the single-channel calculation cannot reproduce the experimental data if any values of λ_w are taken. This means that the real part of the dynamical polarization potential for the ground state is not small in the single-channel calculation. For higher neutron incident energies, we have discussed the case of ^{6}Li $+$ n reactions in Ref. [13]. It was found that the required normalization factor λ_w is much larger, $\lambda_w = 1.5$ for 150 MeV, from the analyses of the total cross section.

For inelastic scattering, Fig. 4 shows the angular distributions to the $7/2^-$ resonance state of ^{7}Li for $E_n = 11.5$, 13.0, 14.1, 18.0, and 24.0 MeV. The calculated cross sections are obtained by integrating the breakup cross section to the $7/2^-$ continuum for the resonance energy region. One sees that the CDCC calculation can also reproduce the inelastic observed cross section. Two-channel calculations (dashed line) include behavior similar to the full-channel ones (solid line), but with different increase in lower incident energies.

In Fig. 5, the calculated neutron spectra are compared with the experimental data at selected angles in the laboratory frame for 11.5 and 18.0 MeV incident energies. Components of ^3P, ^1P, ^1S, ^3D, ^5D, ^7F, and, ^5F are represented by the dash-dotted, dotted, dashed, and thin solid lines, respectively, and these results are broadened by considering the finite resolution of the experimental apparatus [3]. Three peaks in the experimental data represent the elastic, inelastic to the $7/2^-$ resonance, and inelastic to the $5/2^-$ resonance components, respectively, from higher neutron energies. It is important to reproduce the breakup neutron spectrum of ^{7}Li because, first of all, it leads to the tritium production reaction of ^{7}Li, and secondly neutron slow-down by it enhances the tritium production reaction of ^{6}Li, which has a large cross section at low energies. The CDCC calculation gives good agreement with experimental data at the higher neutron energy region. On the other hand in the low neutron energy region, which corresponds to high excited states of ^{7}Li and four-body breakup channels such as $2n + d + \alpha$, the calculated cross section underestimates the experimental data for all energies and angles.

IV. SUMMARY

We analyze the effect of the breakup channel in the elastic and inelastic neutron scattering of ^{7}Li reactions by using the CDCC method with the complex Jeukenne-Lejeune-Mahaux effective nucleon-nucleon interaction. In the present analysis, it is found that the elastic cross sections for incident energies between 11.5 and 24.0 MeV can be reproduced by the present analysis with one normalization parameter for the imaginary part of the JLM interaction ($\lambda_w = 0.1$), and breakup effects on the elastic cross section are significant. Furthermore, the calculated inelastic cross section to the $7/2^-$ resonance state and neutron spectra are also good agreement with the experimental data systematically. Thus, the CDCC method with the JLM interaction is expected to be indispensable for data evaluation of the ^{7}Li(n, n') reactions, and the advantage is to obtain not only elastic and inelastic cross sections but also neutron spectra within the same framework. The n $+$ ^{6}Li model for ^{7}Li is still an open problem in the n $+$ ^{7}Li reaction for analyzing the higher excitation energy of ^{7}Li. We are also interested in investigating higher neutron incident energy region with present calculations compared with the data libraries. These results will be reported in a forthcoming paper.

ACKNOWLEDGMENTS

We would like to thank the members of the nuclear theory group at Hokkaido University. This work was supported by JSPS Asia and Africa Science Platform Program.

[1] W. A. Fowler, Rev. Mod. Phys. **56**, 149 (1984).
[2] Fusion Evaluated Nuclear Data Library, FENDL 3.0E, IAEA, http://www-nds.iaea.org/fendl3/.
[3] M. Ibaraki *et al.*, J. Nucl. Sci. Technol. **35**, 843 (1998).
[4] S. Chiba *et al.*, Phys. Rev. C **58**, 2205 (1998).
[5] S. Chiba, M. Baba, N. Yabuta, T. Kikuchi, M. Ishikawa, N. Hirakawa, and K. Sugiyama, in Proceedings of the International Conference on Nuclear Data for Science and Technology, (Mito, 1988), p. 253, http://wwwndc.jaea.go.jp/1988Mito/.
[6] H. H. Hogue, P. L. von Hehren, D. W. Glasgow, S. G. Glendinning, P. W. Lisowski, C. E. Nelson, F. O. Purser, W. Tornow, C. R. Gould, and L. W. Seagondollar, Nucl. Sci. Eng. **69**, 22 (1979).
[7] L. F. Hansen, J. Rapaport, X. Wang, F. A. Barrios, F. Petrovich, A. W. Carpenter, and M. J. Threapleton, Phys. Rev. C **38**, 525 (1988).
[8] S. Chiba, T. Fukahori, K. Shibata, B. Yu, and K. Kosako, Fusion Eng. Des. **37**, 175 (1997).

[9] T. Fukahori, S. Chiba, N. Kishida, M. Kawai, Y. Oyama, and A. Hasegawa, in *Proceedings of the International Conference on Nuclear Data for Science and Technology*, Trieste, Italy, 1997 (Societa Italiana di Fisica, Bologna, 1997), p. 899.
[10] M. Kamimura, M. Yahiro, Y. Iseri, Y. Sakuragi, H. Kameyama, and M. Kawai, Prog. Theor. Phys. Suppl. **89**, 1 (1986); M. Yahiro, N. Nakano, Y. Iseri, and M. Kamimura, Prog. Theor. Phys. **67**, 1467 (1982).
[11] Y. Sakuragi, M. Yahiro, and M. Kamimura, Prog. Theor. Phys. **89**, 136 (1986); **70**, 1047 (1983).
[12] Y. Hirabayashi and Y. Sakuragi, Phys. Rev. Lett. **69**, 1892 (1992).
[13] T. Matsumoto, D. Ichinkhorloo, Y. Hirabayashi, K. Katō, and S. Chiba, Phys. Rev. C **83**, 064611(R) (2011).
[14] J.-P. Jeukenne, A. Lejeune, and C. Mahaux, Phys. Rev. C **16**, 80 (1977).
[15] A. M. Moro, J. M. Arias, J. Gómez-Camacho, I. Martel, F. Pérez-Bernal, R. Crespo, and F. Nunes, Phys. Rev. C **65**, 011602(R) (2001).
[16] T. Matsumoto, T. Kamizato, K. Ogata, Y. Iseri, E. Hiyama, M. Kamimura, and M. Yahiro, Phys. Rev. C **68**, 064607 (2003).
[17] T. Egami, K. Ogata, T. Matsumoto, Y. Iseri, M. Kamimura, and M. Yahiro, Phys. Rev. C **70**, 047604 (2004).
[18] E. Hiyama, Y. Kino, and M. Kamimura, Prog. Part. Nucl. Phys. **51**, 223 (2003).
[19] S. Saito, Prog. Theor. Phys. **41**, 705 (1969).
[20] R. J. Spiger and T. A. Tombrello, Phys. Rev. **163**, 964 (1967).
[21] M. Takashina and Y. Kanada-En'yo, Phys. Rev. C **77**, 014604 (2008).
[22] N. Keeley and V. Lapoux, Phys. Rev. C **77**, 014605 (2008).
[23] Y. Hirabayashi, Phys. Rev. C **44**, 1581 (1991).